Pure Appl. Chem., Vol. 85, No. 4, pp. 649–659, 2013.
http://dx.doi.org/10.1351/PAC-CON-12-08-04

Multiple bonds between lead atoms and short bonds between transition metals*

Shigeru Nagase

Fukui Institute for Fundamental Chemistry, Kyoto University, Takanonishihiraki-cho 34-3, Sakyo-ku, Kyoto 606-8103, Japan

Abstract: The heaviest analogues of alkynes are investigated to realize a short triple bond between Pb atoms. For a short double bond between Pb atoms, the Pb_2 molecule stabilized by dative *N*-heterocyclic carbenes is investigated. For unsupported and supported short bonds between transition metals, two-coordinate transition-metal and bicyclic four-membered ring complexes are investigated.

Keywords: alkynes; computational chemistry; main-group atoms; multiple bonds; organometallic chemistry; short bonds; transition metals.

INTRODUCTION

Carbon–carbon double and triple bonds play important roles in many fields of chemistry. It is of great interest to replace the carbon atoms with heavier atoms. Although it was once thought that heavier atoms were unable to form multiple bonds, remarkable progress has been made for heavier double bonds [1]. In contrast, heavier triple bonds are still important synthetic targets. The heavier analogues of alkynes, REER (E = Si, Ge, Sn, Pb), have attracted special interest in main-group element chemistry [1]. Accordingly, all the heavier analogues have been synthesized and isolated: $R^{Si}SiSiR^{Si}$ (R^{Si} = $Si^iPr\{CH(SiMe_3)_2\}_2$) [2], BbtSiSiBbt [Bbt = C_6H_2-2,6-$\{CH(SiMe_3)_2\}_2$-4-$C(SiMe_3)_3$] [3], Ar'GeGeAr' [Ar' = C_6H_3-2,6-(C_6H_3-2,6-$^iPr_2)_2$] [4], BbtGeGeBbt [5], Ar'SnSnAr' [6], and Ar*PbPbAr* [Ar* = C_6H_3-2,6-(C_6H_2-2,4,6-$^iPr_3)_2$] [7]. Theoretical calculations have shown that bulky substituent groups play an important role in making the heavier analogues synthetically accessible and isolable as stable compounds [8]. As revealed by X-ray crystal analysis, all the heavier analogues have a *trans*-bent core skeleton [9], unlike the alkyne case. The Si–Si bond distances of $R^{Si}SiSiR^{Si}$ and BbtSiSiBbt are shorter than typical Si–Si double-bond distances, while the Ge–Ge and Sn–Sn bond distances of Ar'GeGeAr', BbtGeGeBbt, and Ar'SnSnAr' are close to Ge–Ge and Sn–Sn double-bond distances.

In contrast, the X-ray crystal structure of the heaviest analogue, Ar*PbPbAr*, has shown that *trans*-bending is increased greatly and the Pb–Pb bond distance is much longer than Pb–Pb single-bond distances [7]. Theoretical calculations have revealed that Ar*PbPbAr* has no π bond between Pb atoms [10]. This exceptional singly bonded structure is ascribed to the fact that the heaviest Pb atom has the strongest tendency to preserve the valence 6s electrons as a lone pair in making bonds [1,7]. It has been accepted that the heaviest Pb analogues of alkynes take a singly bonded structure, unlike the Si, Ge, and Sn cases. In this context, it is important to investigate whether short multiple bonds are formed between Pb atoms. Furthermore, very short bonds between transition metals are investigated, which are assisted by heavier main-group atoms.

Pure Appl. Chem.* **85, 633–849 (2013). A collection of invited papers based on presentations at the 10th International Conference on Heteroatom Chemistry (ICHAC-10), Kyoto, Japan, 20–25 May 2012.

RESULTS AND DISCUSSION

Heaviest analogues of alkynes: RPbPbR

It is convenient to view REER as consisting of two ER components. ER has a ground doublet and excited quartet states. As E becomes heavier, the ground doublet state becomes more stable than the quartet state. Therefore, the doublet–doublet interaction is most preferred for the heaviest case (E = Pb). Two interaction modes (**a** and **b**) between two PbR components in the ground doublet state are presented in Fig. 1. Mode **a** engenders a triply bonded structure [11] because the donor–acceptor interaction of lone-pair electrons is allowed to form two dative bonds between Pb atoms. Mode **b** engenders a singly bonded structure because the lone pair of PbR does not participate in bonding. The lone-pair orbital of PbR is mostly composed of the 6s orbital of Pb. Because of the so-called relativistic effect, the 6s orbital shrinks and is stabilized. Therefore, mode **a** is expected to be less favorable than mode **b**.

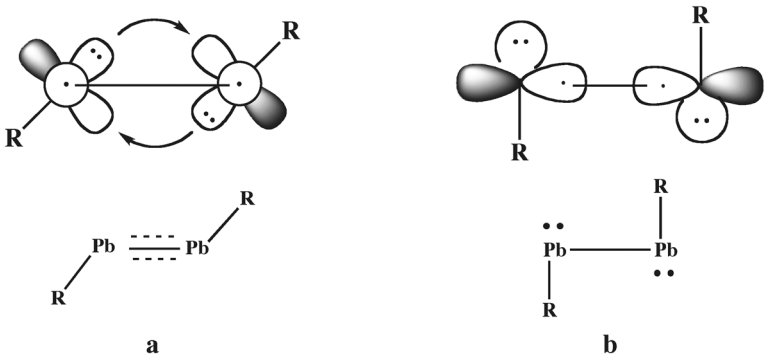

Fig. 1 Two interaction modes between the doublet states of PbR.

The singly bonded structure of Ar*PbPbAr* determined using X-ray crystal analysis was optimized using density functional calculations [12]. The optimized structure is presented in Fig. 2, which has C_2 symmetry. The Pb–Pb bond distance and Pb–Pb–Ar* *trans*-bent angle (θ) are, respectively, 3.260 Å and 100.4º. These agree reasonably well with the experimental values of 3.188 Å and 94.3º in the crystal structure, despite packing forces. The core skeleton is nearly planar, as indicated by the Ar*–Pb–Pb–Ar* dihedral angle (ω) of 175.2º.

The highest occupied molecular orbital (HOMO) and lowest unoccupied molecular orbital (LUMO) of the singly bonded structure respectively correspond to in-plane antibonding π_{in}* and out-of-plane bonding π_{out} orbitals. It is interesting that a new structure with C_2 symmetry is located as an energy minimum by switching the HOMO and LUMO, which is also presented in Fig. 2. The newly located structure is much less *trans*-bent (θ = 117.7º) and has shorter Pb–Pb bond distance of 3.071 Å, although it is 119.8º twisted around the Pb–Pb bond because of the bulk of the Ar* group. The new structure corresponds to a triply bonded structure, because the Pb–Pb bond consists of a σ bond, a somewhat distorted π_{out} bond, and a slipped π_{in} bond [12]. The triply bonded structure is 1.0 kcal/mol more stable than the singly bonded structure.

The energy difference favoring the triply bonded structure is small. However, UV–vis spectra provide important information. For Ar*PbPbAr*, two absorptions with different intensities have been observed at 397 nm (ε = 29 000) and 719 nm (ε = 5200) in *n*-hexane solution [7], as in the cases of Ar'GeGeAr' (371 and 501 nm) [4] and Ar'SnSnAr' (410 and 597 nm) [6]. The two absorptions are well reproduced as 413 nm (f = 0.141) and 822 nm (f = 0.025) by calculations on the triply bonded structure [13], although only one strong absorption is calculated at 416 nm (f = 0.383) for the singly bonded structure. These results indicate that Ar*PbPbAr* has a triply bonded structure in solution.

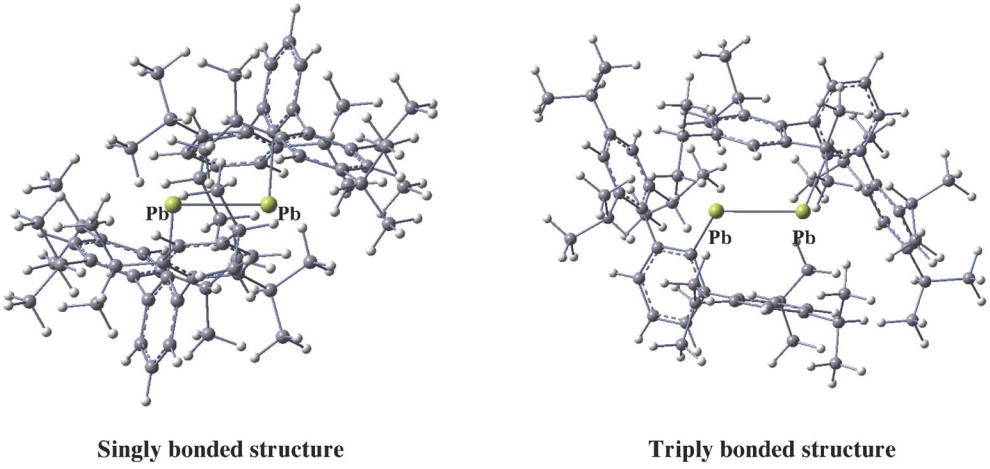

Fig. 2 Singly and triply bonded structures optimized for Ar*PbPbAr*.

The Pb analogues of alkenes (R_2PbPbR_2) have been known to dissociate in solution to provide two singlet divalent species (PbR_2) [1,14]. Dissociation of the triply bonded Ar*PbPbAr*, which engenders two PbAr* fragments in the ground doublet state, was calculated to be 12.2 kcal/mol endothermic. For the PbAr* fragment, two weak absorptions with almost equal intensities were calculated at 420 nm (f = 0.026) and 388 nm (f = 0.024), which differ considerably in both absorption positions and intensities from the two absorptions observed (or calculated) for Ar*PbPbAr*. These confirm that Ar*PbPbAr* does not dissociate in solution but that it has a triply bonded structure, unlike the R_2PbPbR_2 case, suggesting that the singly bonded structure in the crystalline results from packing forces. The same is true also for the tin analogues of alkynes with bulky groups [15]. For example, the structure of 4-$SiMe_3$-Ar'SnSnAr'-4-$SiMe_3$ (Ar'-4-$SiMe_3$ = C_6H_2-2,6-(C_6H_3-2,6-$^i Pr_2$)$_2$-4-$SiMe_3$) determined using X-ray crystal analysis [16] corresponds to a singly bonded structure [17]. However, the triply bonded structure is calculated to be 5.4 kcal/mol more stable [15]. Accordingly, the UV–vis spectrum of 4-$SiMe_3$-Ar'SnSnAr'-4-$SiMe_3$ displays two absorptions at 416 and 608 nm that closely resemble those of Ar'SnSnAr' (410 and 597 nm), indicating that 4-$SiMe_3$-Ar'SnSnAr'-4-$SiMe_3$ has a triply bonded structure in solution. These suggest that crystal structures are not very helpful for compounds with bulky groups.

The Pb–Pb bond distance of 3.071 Å calculated for the triply bonded structure of Ar*PbPbAr* is considerably longer than the Pb–Pb single-bond distance of 2.844 Å in $Ph_3PbPbPh_3$. Reportedly for REER, electropositive silyl groups decrease *trans*-bending and shorten the E–E bond distance [3b,8]. Therefore, several bulky silyl groups were tested using density functional calculations. The optimized structure of $R^{Si}PbPbR^{Si}$ (R^{Si} = Si^{i}Pr{$CH(SiMe_3)_2$}$_2$) with θ = 128.9º and ω = 155.6º is depicted in Fig. 3, which has C_2 symmetry. The two Pb atoms are triply bonded, as is shown Fig. 4: one σ bond, one π_{out} bond, and one π_{in} bond (slightly slipped by the mixing of the σ* orbital because of *trans*-bending [9]) exist between the Pb atoms. The Pb–Pb bond distance of 2.696 Å is remarkably shorter than the Pb–Pb single-bond distance of 2.844 Å in $Ph_3PbPbPh_3$. In addition, it is considerably shorter than the shortest Pb–Pb double-bond distance of 2.903 Å known to date for $Si(SiMe_3)_3MesPb{=}PbSi(SiMe_3)_3Mes$ (Mes = C_6H_2-2,4,6-Me_3)[14e]. However, the triply bonded structure was calculated to be 4.3 kcal/mol less stable than the singly bonded structure (Pb–Pb = 3.080 Å, θ = 100.2º, and ω = 134.4º). We are still searching for good substituent groups that stabilize a triply bonded structure with a sufficiently short Pb–Pb bond.

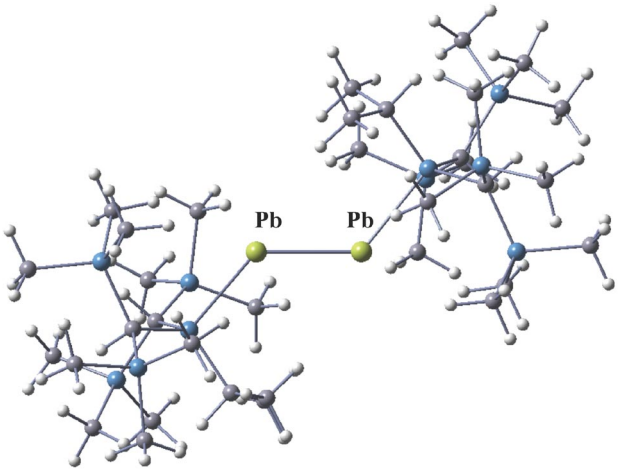

Fig. 3 Triply bonded structure optimized for $R^{Si}PbPbR^{Si}$.

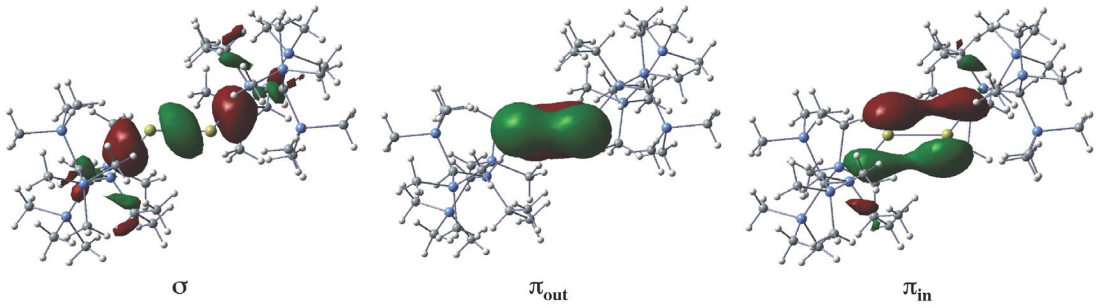

Fig. 4 One σ orbital and two π orbitals between Pb atoms for $R^{Si}PbPbR^{Si}$.

Pb–Pb double bond stabilized by dative carbene ligands

As a new type of double bond, diatomic molecules stabilized by the coordination of dative *N*-heterocyclic carbenes (NHCs) are of interest currently [18]. Stabilization was performed by synthesis and isolation of L: → Si=Si ← :L (L = :C[N(2,6-$^{i}Pr_2$-C_6H_3)CH]$_2$) [19]. In addition, L: → Ge=Ge ← :L was also synthesized and isolated [20]. The Si and Ge atoms are regarded as being in a formal zero-oxidation state. The Si–Si and Ge–Ge bond distances compare well with typical double bond distances of $R_2Si=SiR_2$ and $R_2Ge=GeR_2$.

Because the heaviest Pb case remains unknown [21], the optimized structure of L: → Pb=Pb ← :L is presented in Fig. 5a, which has C_{2h} symmetry. The two Pb atoms are doubly bonded. As Fig. 6 shows, one σ bond and one π bond exist between the Pb atoms. It is notable that the Pb–Pb double-bond distance of 2.833 Å is considerably shorter than the shortest Pb–Pb double-bond distance of 2.903 Å known to date [14e] and differs little from the Pb–Pb bond distance of Pb_2. As Fig. 5b shows, L: → Pb=Pb ← :L is formed by the donation of the lone pair of L: into the vacant 6p orbital on Pb [22]. Therefore, the Pb–Pb–L bond angle of 93.0º is close to 90º. The electron donation from L: makes the Pb atom negatively charged slightly (the charge on Pb is –0.17). The L–Pb–Pb–L linkage is expected to become linear for the formal +2 oxidation state of the Pb atom [23]. The linear structure with a planar L:PbPbL: core is calculated to be 21.3 kcal/mol less stable and does not correspond to an energy minimum [24]. The binding energy between Pb_2 ($^3\Sigma_g^-$) and 2L: is calculated to be 45.6 kcal/mol. This

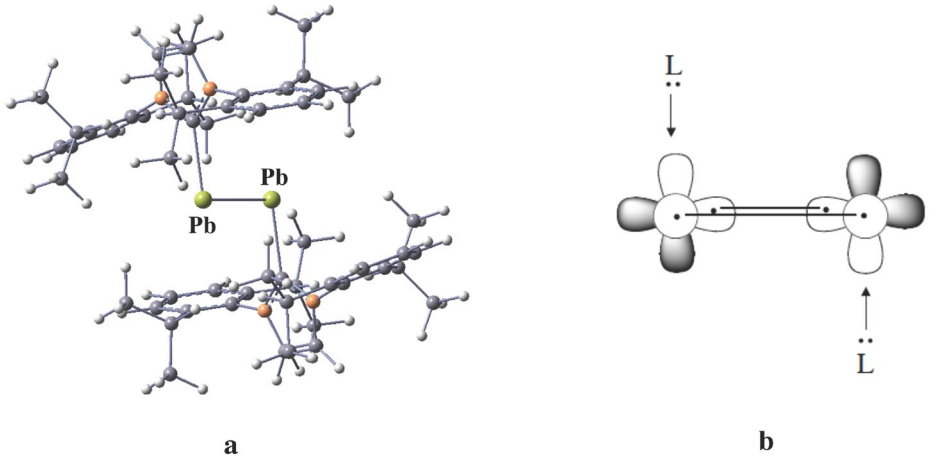

Fig. 5 (a) Optimized structure of L: → Pb=Pb ← :L. (b) Donation of the lone pair of :L into the vacant 6p orbital of the Pb atom (for simplicity, the 6s orbital of Pb is omitted).

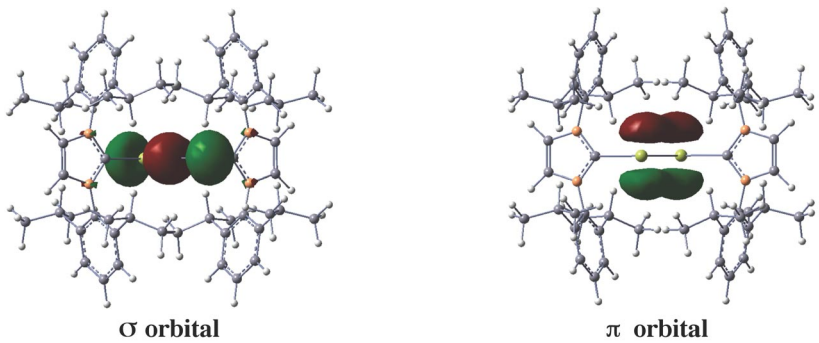

Fig. 6 σ and π orbitals between Pb atoms for L: → Pb=Pb ← :L.

value is smaller than the value of 80.9 kcal/mol calculated for the simplified L: → Si=Si ← :L (where L: is :C[N(Me)CH]$_2$) [19], because of the higher-lying vacant 6p orbital on Pb and the larger singlet ($^1\Delta_g$)-triplet ($^3\Sigma_g^-$) energy difference [25] of Pb_2. However, L: → Pb=Pb ← :L is expected to be an interesting synthetic target.

Short bonds between transition metals

The most common coordination numbers for complexes of transition metals are four, five, and six. As novel transition-metal complexes with an unsupported two-coordinate metal, R*MFe(η^5-C_5H_5)$(CO)_2$ (M = Fe, Mn, Cr; R* = C_6H-2,6-Ar_2-3,5-^{i}Pr$_2$ where Ar = C_6H_2-2,5,6-^{i}Pr$_3$) has recently been synthesized and isolated [26,27]. As is shown in Fig. 7, the bulky R* group surrounds the two-coordinate M atom and blocks the formation of any third bond to M. X-ray crystal analysis shows that the metal–metal bond distances are 2.393 Å for Fe–Fe, 2.451 Å for Mn–Fe, and 2.489 Å for Cr–Fe. These bonds are much shorter than those of the known complexes with unsupported Fe–Fe (2.687–3.138 Å), Mn–Fe (2.601–2.843 Å), and Cr–Fe (2.901–2.957 Å) bonds, suggesting that R*MFe(η^5-C_5H_5)$(CO)_2$ has the shortest unsupported metal–metal bond. The Fe–Fe and Mn–Fe bond distances of R*MFe(η^5-C_5H_5)$(CO)_2$ determined using X-ray crystal analysis are very close to the values of 2.403 Å (Fe–Fe) and 2.458 Å (Mn–Fe) obtained by density functional calculations. It was calculated that the Fe–Fe bond

distance is shortened to 2.362 Å upon the replacement of the R* group by the much smaller Ph group, which suggests that the Fe–Fe bond distance of R*FeFe(η^5-C_5H_5)$(CO)_2$ is elongated somewhat by the bulky R* group. It was indicated that the near-linear structure at the two-coordinate Fe atom is attributable to the bulk of the R* group [27]. However, it is calculated that PhFeFe(η^5-C_5H_5)$(CO)_2$ has a much more linear structure (176.6º) than R*FeFe(η^5-C_5H_5)$(CO)_2$ [166.5º (cal) or 163.9º (exp)].

The optimized structure of R*FeFe(η^5-C_5H_5)$(CO)_2$ is portrayed in Fig. 7b. The two-coordinate Fe atom is paramagnetic, with the largest spin density of 3.8. The four singly occupied molecular orbitals (SOMOs) of R*FeFe(η^5-C_5H_5)$(CO)_2$ consisting mostly of d orbitals are highly localized on the two-coordinate Fe atom, as presented in Fig. 8. These are consistent with results of a magnetic study that suggest the quintet ground state [26]. Dissociation of R*FeFe(η^5-C_5H_5)$(CO)_2$, which leads to ground quartet R*Fe and ground doublet Fe(η^5-C_5H_5)$(CO)_2$ states, is 44.2 kcal/mol endothermic [28]. The low Fe–Fe bond order of 0.36 indicates limited covalent interaction between Fe atoms, because the two-coordinate Fe and neighboring Fe atoms are positively (+1.12) and negatively (–1.35) charged greatly, respectively. This is also reflected in the polarized σ orbital between the Fe atoms, as shown in Fig. 9. It can be considered that the σ (Fe–Fe) orbital results from interaction between the singly occupied σ orbitals of the sextet R*Fe and doublet Fe(η^5-C_5H_5)$(CO)_2$ fragments. As Fig. 10 shows, the σ energy level at –5.8 eV for Fe(η^5-C_5H_5)$(CO)_2$ is much lower than that at –3.9 eV for R*Fe. Therefore, the σ (Fe–Fe) orbital is dominated by the σ orbital of Fe(η^5-C_5H_5)$(CO)_2$. The σ (Fe–Fe) orbital is doubly occupied by accepting one electron from R*Fe. Therefore, it contributes to the charge distribution of $R^*Fe^{+1.12}Fe^{-1.35}$(η^5-C_5H_5)$(CO)_2$. Another view is that one electron is first transferred from the high-lying σ orbital of R*Fe into the low-lying σ orbital of Fe(η^5-C_5H_5)$(CO)_2$; two electrons paired in the σ orbital of Fe(η^5-C_5H_5)$(CO)_2$ are donated into the emptied σ orbital of R*Fe. In this view, the Fe–Fe bond is regarded as a dative bond [26].

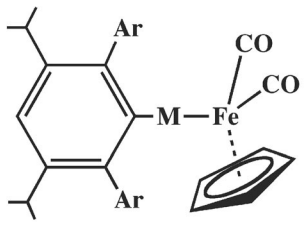

a

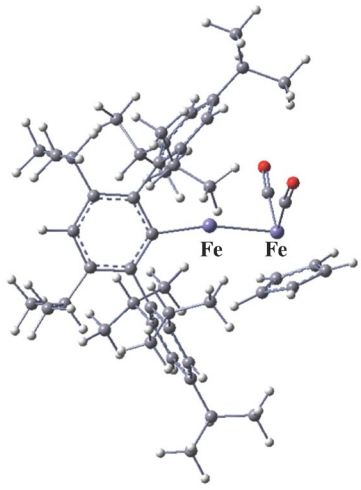

b

Fig. 7 (a) R*MFe(η^5-C_5H_5)$(CO)_2$. (b) Optimized structure of R*FeFe(η^5-C_5H_5)$(CO)_2$.

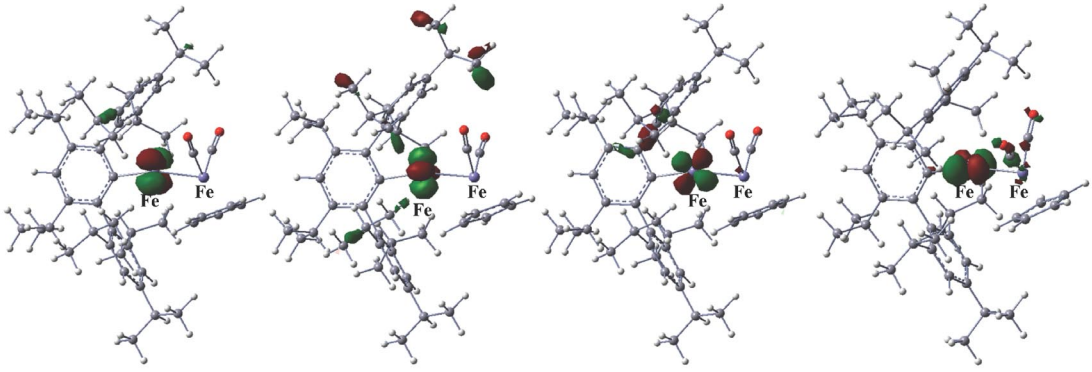

Fig. 8 Four SOMOs of R*FeFe(η^5-C_5H_5)$(CO)_2$.

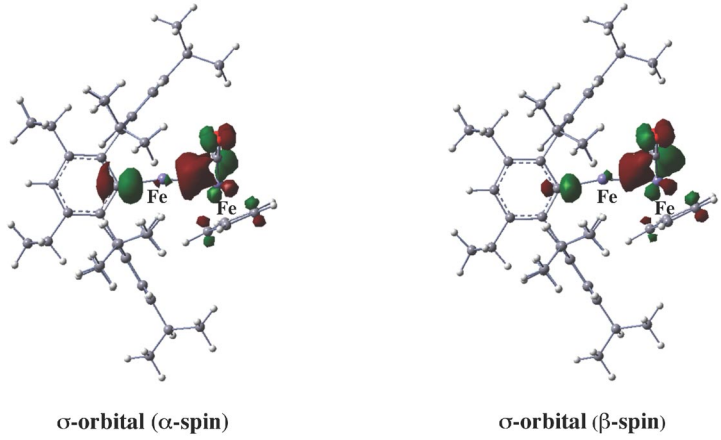

Fig. 9 α-spin and β-spin σ orbitals between Fe atoms for R*FeFe(η^5-C_5H_5)$(CO)_2$.

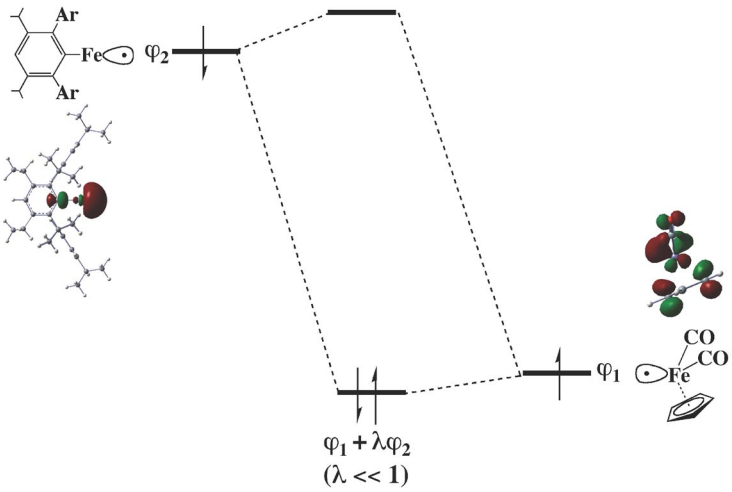

Fig. 10 Orbital interaction between R*Fe and Fe(η^5-C_5H_5)$(CO)_2$.

Calculations show that the Fe–Fe bond distance is greatly shortened in the bicyclic four-membered ring presented in Fig. 11a. It is remarkable that the Fe–Fe bond distance of 2.045 Å is much shorter than the shortest Fe–Fe bond distance of 2.198 Å reported to date [29]. The bond shortening assisted by two Sn atoms was very recently performed for the bicyclic four-membered Ru_2Sn_2 ring complex [30] presented in Fig. 11b. The Ru–Ru bond distance of 2.343 Å determined through X-ray crustal analysis agrees well with the calculated value of 2.363 Å. It is shorter than the Ru–Ru distance of 2.449–2.469 Å in the related bridge complexes, for which it is assumed that the two Ru atoms are triply bonded [31]. As shown in Fig. 12, localized molecular orbital analysis reveals that one clear σ bond exists between the Ru atoms, while two three-centered σ orbitals are delocalized over each of the three-membered Ru_2Sn rings, which make an important contribution to Ru–Ru bonding. As a result, the Ru–Ru bond has a somewhat multiple-bond character, as indicated by the bond order of 1.3.

It is also predicted that the Ru–Ru bond distance in the bicyclic four-membered ring is shortened further in the bicyclic six-membered Ru_2Sn_4 ring, although the shortening does not take place for the corresponding Ru_2C_4 ring. Experimental confirmation is in progress.

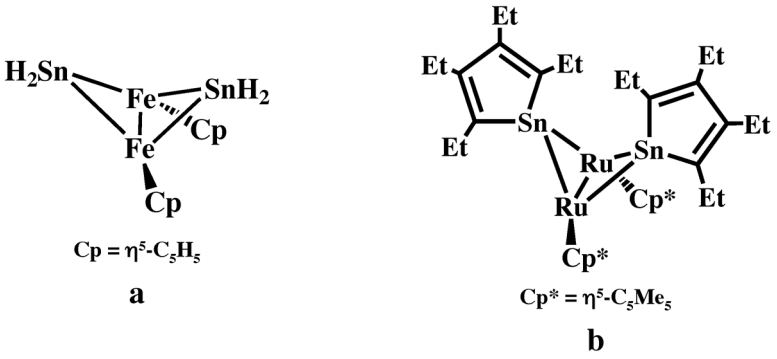

Fig. 11 Bicyclic four-membered ring complexes with (a) Fe_2Sn_4 and (b) Ru_2Sn_4 cores.

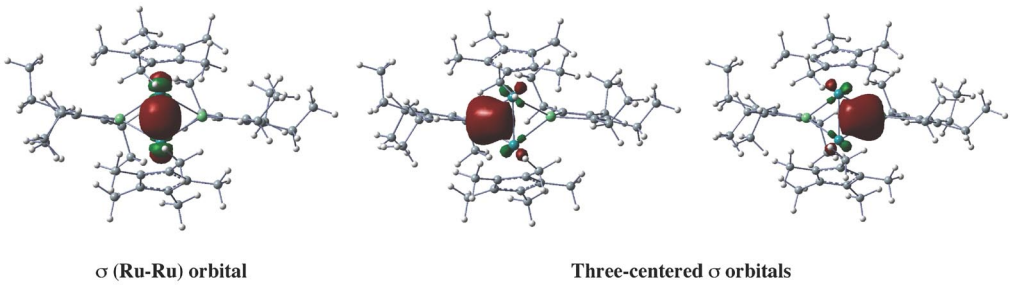

Fig. 12 One σ orbital between Ru atoms and two three-centered σ orbitals delocalized over the three-membered rings for the complex presented in Fig. 11b.

CONCLUDING REMARKS

It remains an important subject whether the heaviest analogues of alkynes are synthesized and isolated as stable compounds with a sufficiently short Pb–Pb triple bond. The Pb_2 molecule stabilized by dative carbene ligands is an interesting synthetic target. It enriches the chemistry of heavier double bonds, while short metal–metal bonds assisted by heavier main-group atoms enrich the chemistry of transition-

metal complexes. Close interplay between calculations and experiment is important to develop interesting bonds, structures, and reactions.

COMPUTATIONAL METHODS

Calculations were conducted using the Gaussian 09 program [32]. For Ar*PbPbAr*, $R^{Si}PbPbR^{Si}$, and L: → Pb=Pb ← :L, geometries were optimized using hybrid density functional theory at the B3PW91 [33,34] level. The triple zeta basis set (obtained from the double zeta LANL2DZ [35] basis set) augmented by two sets of d polarization functions (d exponents 0.213 and 0.062) and the relativistic effective core potential [35] were used for Pb, while the 6-31G(d) [36] basis set was used for other atoms. Excitation energies were calculated using the time-dependent (TD)-B3PW91 method. For R*MFe(η^5-C_5H_5)$(CO)_2$, geometries were optimized using the spin-unrestricted B3LYP [33,37] method. The LANL2DZ basis set and the effective core potential were used for M; the 6-31G (d) basis set was used for other atoms. For bicyclic Ru_2Sn_2 complexes, geometries were optimized at the B3PW91 level. The LANL2DZ basis set was augmented by d polarization functions (d exponent 0.186) for Sn and f polarization functions (f exponent 1.234) for Ru; the 6-31G(d) basis set was used for other atoms.

ACKNOWLEDGMENTS

The author is grateful to Drs. J.-D. Guo and N. Takagi for theoretical calculations, to Prof. P. P. Power for the joint research of R*MFe(η^5-C_5H_5)$(CO)_2$, and to Prof. M. Saito for joint research related to bicyclic Ru_2Sn_2 complexes. This work was supported in part by a Grant-in-Aid for Creative Scientific Research and Specially Promoted Research from the Ministry of Education, Culture, Sports, Science, and Technology (MEXT) of Japan.

REFERENCES AND NOTES

1. For a recent review, see: R. C. Fischer, P. P. Power. *Chem. Rev*. **110**, 3877 (2010).
2. A. Sekiguchi, R. Kinjo, M. Ichinohe. *Science* **305**, 1755 (2004).
3. (a) T. Sasamori, K. Hironaka, Y. Sugiyama, N. Takagi, S. Nagase, Y. Hosoi, Y. Furukawa, N. Tokitoh. *J. Am. Chem. Soc*. **130**, 13856 (2008); (b) T. Sasamori, J. S. Han, K. Hironaka, N. Takagi, S. Nagase, N. Tokitoh. *Pure Appl. Chem.* **82**, 603 (2010).
4. (a) M. Stender, A. D. Phillips, R. J. Wright, P. P. Power. *Angew. Chem., Int. Ed.* **41**, 1785 (2002); (b) L. Pu, A. D. Phillips, A. F. Richards, M. Stender, R. S. Simons, M. M. Olmstead, P. P. Power. *J. Am. Chem. Soc.* **125**, 11626 (2003).
5. Y. Sugiyama, T. Sasamori, Y. Hosoi, Y. Furukawa, N. Takagi, S. Nagase, N. Tokitoh. *J. Am. Chem. Soc*. **128**, 1023 (2006).
6. A. D. Phillips, R. J. Wright, M. M. Olmstead, P. P. Power. *J. Am. Chem. Soc.* **124**, 5930 (2002).
7. L. Pu, B. Twamley, P. P. Power. *J. Am. Chem. Soc.* **122**, 3524 (2000).
8. (a) K. Kobayashi, S. Nagase. *Organometallics* **16**, 2489 (1997); (b) S. Nagase, K. Kobayashi, N. Takagi. *J. Organomet. Chem.* **611**, 264 (2000); (c) K. Kobayashi, N. Takagi, S. Nagase. *Organometallics* **20**, 234 (2001); (d) N. Takagi, S. Nagase. *Organometallics* **20**, 5498 (2001); (e) N. Takagi, S. Nagase. *Chem. Lett*. 966 (2001); (f) N. Takagi, S. Nagase. *Eur. J. Inorg. Chem.* 2775 (2002); (g) N. Takagi, S. Nagase. *J. Organomet. Chem.* **692**, 217 (2007).
9. Stabilization of REER due to trans-bending is ascribed to the mixing of the low-lying vacant σ* orbital into the in-plane π_{in} orbital, known as a second-order Jahn–Teller effect. The mixing of the antibonding σ* orbital is enhanced, as the E atom becomes heavier. It makes the bonding π_{in} orbital slipped and weakened.

10. (a) Y. Chen, M. Hartmann, M. Diedenhofen, G. Frenking. *Angew. Chem., Int. Ed.* **40**, 2052 (2001); for a theoretical study of two trans-bent forms of RPbPbR, see also: (b) M. Lein, A. Krapp, G. Frenking. *J. Am. Chem. Soc.* **127**, 6290 (2005).
11. Bond order is often discussed to characterize bond multiplicity and strength, though it is an artificial index. Because the two dative bonds in mode **a** are weak, the Pb–Pb bond order is less than three. However, we prefer to call the Pb–Pb bond a triple bond, because there are three bonds between the Pb atoms. Bond order is not always correlated to bond strength, unlike the carbon cases.
12. N. Takagi, S. Nagase. *Organometallics* **26**, 3627 (2007).
13. It should be described that the energy of the triply bonded structure of Ar*PbPbAr* is not sensitive to the dihedral angle (ω). For example, the structure optimized by fixing the angle at $\omega = 140°$ is only 0.7 kcal/mol less stable than the fully optimized structure ($\omega = 119.8°$). The two absorptions of 420 and 752 nm calculated for $\omega = 140°$ are closer to the experimental values of 397 and 719 nm.
14. (a) K. W. Klinkhammer, T. F. Fässler, H. Grützmacher. *Angew. Chem., Int. Ed.* **37**, 124 (1998); (b) M. Stürmann, M. Weidenbruch, K. W. Klinkhammer, F. Lissner, H. Marsmann. *Organometallics* **17**, 4425 (1998); (c) M. Stürmann, W. Saak, H. Marsmann, M. Weidenbruch. *Angew. Chem., Int. Ed.* **38**, 187 (1999); (d) M. Stürmann, W. Saak, M. Weidenbruch, K. W. Klinkhammer. *Eur. J. Inorg. Chem.* 579 (1999); (e) K. Klinkhammer. *Polyhedron* 587 (2002); (f) S. Hino, M. Olmstead, A. D. Phillips, R. J. Wright, P. P. Power. *Inorg. Chem.* **43**, 7346 (2004).
15. N. Takagi, S. Nagase. *Organometallics* **26**, 469 (2007).
16. R. C. Fischer, L. Pu, J. C. Fettinger, M. A. Brynda, P. P. Power. *J. Am. Chem. Soc*. **128**, 11366 (2006).
17. For other examples, see: Y. Peng, R. C. Fischer, W. A. Merrill, J. Fischer, L. Pu, B. D. Ellis, J. C. Fettinger, R. H. Herber, P. P. Power. *Chem. Sci*. **1**, 461 (2010).
18. For recent reviews, see: (a) Y. Wang, G. H. Robinson. *Inorg. Chem*. **50**, 12326 (2011); (b) Y. Wang, G. H. Robinson. *Dalton Trans*. **41**, 337 (2012).
19. Y. Wang, Y. Xie, P. Wei, R. B. King, H. F. Schaefer III, P. v. R. Schleyer, G. H. Robinson. *Science* **321**, 1069 (2008).
20. A. Sidiropoulos, C. Jones, A. Stasch, S. Klein, G. Frenking. *Angew. Chem., Int. Ed*. **48**, 9701 (2009).
21. For the P_2 case, see: (a) Y. Wang, Y. Xie, P. Wei, R. B. King, H. F. Schaefer III, P. v. R. Schleyer, G. H. Robinson. *J. Am. Chem. Soc*. **130**, 14970 (2008); for the As_2 case, see: (b) M. Y. Abraham, Y. Wang, Y. Xie, P. Wei, H. F. Schaefer III, P. v. R. Schleyer, G. H. Robinson. *Chem.—Eur. J*. **16**, 432 (2010); for the B_2 case, see: (c) H. Braunschweig, R. D. Dewhurst, K. Hammond, J. Mies, K. Radacki, A. Vargas. *Science* **336**, 1420 (2012); (d) N. Holzmann, A. Stasch, C. Jones, G. Frenking. *Chem.—Eur. J*. **17**, 13517 (2011).
22. The size difference between valence s and p orbitals becomes the largest for the heaviest Pb atom [8b]. Therefore, the Pb atom is most reluctant to form hybrid orbitals. It should be noted in Fig. 5b that no hybrid orbital is required for the Pb atom.
23. C. A. Dyker, G. Bertrand. *Science* **321**, 1050 (2008).
24. For the linear structure, hybrid orbitals are required for the Pb atom.
25. The Pb_2 molecule has the triplet ground state ($^3\Sigma_g^-$), as do Si_2 and Ge_2. For the interaction shown in Fig. 5b, Pb_2 must be excited to the singlet state ($^1\Delta_g$).
26. H. Lei, J.-D. Guo, J. C. Fettinger, S. Nagase, P. P. Power. *J. Am. Chem. Soc*. **132**, 17399 (2010).
27. For a highlight article, see: P. L. Holland. *Angew. Chem., Int. Ed.* **50**, 6213 (2011).
28. Dissociation on the quintet potential energy surface, which leads to excited sextet R*Fe and ground doublet $Fe(\eta^5\text{-}C_5H_5)(CO)_2$ states, is 59.3 kcal/mol endothermic.

29. (a) F. A. Cotton, L. M. Daniels, L. R. Falvello, J. H. Matonic, C. A. Murillo. *Inorg. Chim. Acta* **256**, 269 (1997); (b) F. A. Cotton, L. M. Daniels, J. H. Matonic, C. A. Murillo. *Inorg. Chim. Acta* **256**, 277 (1997); for a significantly shorter Fe–Fe bond distance of 2.127 Å reported recently, see: (c) L. Fohlmeister, S. Liu, C. Schulten, B. Moubaraki, A. Stasch, J. D. Cashion, K. S. Murray, L. Gagliardi, C. Jones. *Angew. Chem., Int. Ed.* **51**, 8294 (2012).
30. T. Kuwabara, M. Saito, J.-D. Guo, S. Nagase. Unpublished results.
31. T. Takao, M. Amako, H. Suzuki. *Organometallics* **22**, 3855 (2003).
32. M. J. Frisch, G. W. Trucks, H. B. Schlegel, G. E. Scuseria, M. A. Robb, J. R. Cheeseman, G. Scalmani, V. Barone, B. Mennucci, G. A. Petersson, H. Nakatsuji, M. Caricato, X. Li, H. P. Hratchian, A. F. Izmaylov, J. Bloino, G. Zheng, J. L. Sonnenberg, M. Hada, M. Ehara, K. Toyota, R. Fukuda, J. Hasegawa, M. Ishida, T. Nakajima, Y. Honda, O. Kitao, H. Nakai, T. Vreven, J. A. Montgomery Jr., J. E. Peralta, F. Ogliaro, M. Bearpark, J. J. Heyd, E. Brothers, K. N. Kudin, V. N. Staroverov, R. Kobayashi, J. Normand, K. Raghavachari, A. Rendell, J. C. Burant, S. S. Iyengar, J. Tomasi, M. Cossi, N. Rega, J. M. Millam, M. Klene, J. E. Knox, J. B. Cross, V. Bakken, C. Adamo, J. Jaramillo, R. Gomperts, R. E. Stratmann, O. Yazyev, A. J. Austin, R. Cammi, C. Pomelli, J. W. Ochterski, R. L. Martin, K. Morokuma, V. G. Zakrzewski, G. A. Voth, P. Salvador, J. J. Dannenberg, S. Dapprich, A. D. Daniels, O. Farkas, J. B. Foresman, J. V. Ortiz, J. Cioslowski, D. J. Fox. *Gaussian 09 (Revision A.01)*, Gaussian, Inc., Wallingford, CT (2009).
33. (a) A. D. Becke. *Phys. Rev*. *A* **38**, 3098 (1988); (b) A. D. Becke. *J. Chem. Phys*. **98**, 5648 (1933).
34. C. Lee, W. Wang, R. G. Parr. *Phys. Rev*. *B* **37**, 785 (1988).
35. (a) W. R. Wadt, P. J. Hay. *J. Chem. Phys*. **82**, 284 (1985); (b) P. J. Hay, W. R. Wadt. *J. Chem. Phys.* **82**, 299 (1985).
36. M. N. Francl, W. J. Pietro, W. J. Hehre, J. S. Binkley, M. S. Gordon, D. J. Defrees, J. A. Pople. *J. Chem. Phys*. **77**, 3654 (1982).
37. J. P. Perdew, Y. Wang. *Phys. Rev*. *B* **45**, 13244 (1922).

